FGF8-mediated signaling regulates tooth growth rate and size during odontogenesis

Chensheng Lin, Ningsheng Ruan, Linjun Li, Yibin Chen, Xiaoxiao Hu, Xuefeng Hu*, Yanding Zhang*

Fujian Key Laboratory of Developmental and Neural Biology & Southern Center for Biomedical Research, College of Life Sciences, Fujian Normal University, Fuzhou, Fujian, 350117, P.R. China.

* **Corresponding authors:** Xuefeng Hu, +86-13055734898 (tel), bioxfh@fjnu.edu.cn; Yanding Zhang, +86-13706963408 (tel), ydzhang@fjnu.edu.cn

Abstract

The current understanding of the regulatory mechanism of organ growth is almost based on *Drosophila melanogaster*. In the present study, we manipulated heterotypic recombination between human and mouse dental tissues and found that the dental mesenchyme is the principal component to dominate the tooth development rate and size and FGF8 could be a critical player in this process. Forced activation of dental mesenchymal *Fgf8* signaling in mice promotes the transition of the cell cycle from G1 to S -phase via p38 and perhaps PI3K-Akt intracellular signaling, resulting in promotion of cell proliferation and prevention of cell apoptosis, and thus slowdown the tooth growth rate and enlarge the tooth size. Our results provide evidences, for the first time to our knowledge, that dental mesenchymal FGF8 may be a critical intrinsic factor in controlling tooth growth rate and size during mammalian odontogenesis.

Key words: FGF8, tooth, growth rate, size, human, mouse.

Introduction

Although mammals possess an almost identical body plan with morphologically and functionally similar organs and systems, their life span and body sizes vary greatly among different species. Generally, larger-bodied species own longer gestation lengths and life spans with slower development process to acquire larger organ sizes [1, 2]. The mechanisms that regulate organismal growth rate and body size have been well investigated in non-mammalian models, particularly in *Drosophila melanogaster*, in which roles of TOR (target of rapamycin), insulin/IGF (insulin-like growth factor), Ras/Raf/MAPK, JNK (c-Jun N-terminal kinase), and Hippo signaling pathways are well defined [3].

In mammals, several conserved families, including FGF (fibroblast growth factor), BMP (bone morphogenetic protein), TGF-β (transforming growth factor-β), GH (growth hormone)/IGF, Hippo/YAP, and Akt/mTOR, are deemed to be involved in the regulation of organismal growth rate and body size due to their ability to modulate cell proliferation and apoptosis during embryonic development [3-5]. Among these pathways, the Hippo signaling has been verified to play its best-known physiological function, the regulation of cell proliferation and apoptosis and thereby cell number, on organ size in the mouse model for mammalian lineage[6-10]. However, no direct evidences can explain roles of pathways abovementioned in controlling organ growth rate and body size, except for the Hippo pathway, in mammals; even so, augmented Hippo signaling has been reported to induce organ enlargements only in the liver, stomach, heart, and spleen, but not kidney, lung, and intestine [11-13], suggesting that organs adopt different strategies

for controlling their development rates and organ sizes in mammals.

Mammalian teeth have long served as a model organ for studying fundamental questions in organ development on the molecular basis [14]. The main features of tooth morphogenesis are conserved in the mammalian lineage [15-17], as they are all formed by sequential and reciprocal interactions between epithelium and mesenchyme and share similar processes during tooth development [16]. Despite these considerable homologies, mammalian dentition undergoes remarkable morphological diversification, displaying great variations not only in tooth shape and number but also tooth size and growth rate [14, 16, 18-20]. Obviously, the human dentition appears much larger size than the mouse one. In addition, the period of tooth developmental process in humans takes about 400 days from the initiation stage at embryonic 6th week to tooth eruption at postnatal 6th month. Whereas, the period of this process in mice takes only about 20 days from the determination of tooth forming sites at E10.5 to tooth eruption at postnatal 10th day [14]. The regulatory mechanism of tooth growth rate and size in mammals is still unknown. Studies in mice demonstrated that the function of the Hippo pathway, the only known signaling pathway that controls organ size in mammals, does not involve in the regulation of tooth growth rate and size during mammalian odontogenesis [7, 21].

It is generally believed that diversified forms of organ morphogenesis (including growth rate and size) among species are achieved by tinkering conserved signaling pathways instead of proposing novel ones during development [22-24]. The difference in organismal growth rate and organ or body size between human and mouse primarily reflect the difference in cell number rather than the cell size [25]. Ample evidences from

mouse models demonstrate that numerous growth factors of conserved families, such as FGF, BMP, SHH, and Wnt, have been shown to play critical roles in tooth morphogenesis by regulating cell proliferation, differentiation, and apoptosis during odontogenesis [16, 17, 23, 26-30]. Here, we provide strong evidences that mesenchymal FGF8 may act as a critical intrinsic factor in controlling tooth development rate and size during mammalian odontogenesis. FGF8 signaling, via activation of p38 and perhaps PI3K-Akt intracellular pathways, promotes cell cycle from G1- to S-stage transition and gives rise to the increase of cell proliferation and the decrease of cell apoptosis, thus resulting in prolonged tooth development phase and enlarged tooth size in mammals.

Results

Tooth growth rate and size is dominated by dental mesenchyme in humans and mice.

Our previous studies have showed that epithelial sheets of human keratinocyte stem cells, when recombined with E13.5 mouse dental mesenchyme, can be induced to differentiate into enamel-secreting ameloblasts in only 10 days and apoptotically degraded in 4 weeks to achieve small-sized chimeric teeth with similar size to mouse ones, whereas the mouse second branchial arch epithelium, when recombined with human dental mesenchyme from the bell-stage, remains in an enamel-secreting status after 15-week *ex vivo* culture and acquired large-sized teeth in the end, a size similar to human deciduous teeth [31-33]. These results strongly imply that the growth rate and size control in tooth development could be dominated by the mesenchymal component in humans and mice. To validate our hypothesis, we comprehensively revisited these phenotypes by carrying out meticulously designed heterogeneous recombination between human and mouse dental tissues (Table. 1). As shown in Fig. 1a-c, it took more than 4 weeks for mouse dental epithelium to deposit enamel when recombined with human dental mesenchyme in mde+hdm chimeric tooth germs, exhibiting a much longer development phase in comparison with mouse dental epithelium that were combined with their own dental mesenchyme (Fig. 1e-g). By contrast, it took around only 10 days for human dental epithelium to deposit enamel when recombined with E13.5 mouse dental mesenchyme in hde+mdm chimeric tooth germs (Fig. 1i-k), demonstrating a dramatically accelerated development rate compared to the normal

human tooth morphogenesis. When the mouse dental epithelium were recombined with single human dental mesenchyme, in addition to the compliance of growth rate with that of human dental mesenchyme, the chimeric tooth germ generated an enlarged tooth after 16-week growth for sufficient mineralization (Fig. 1d), whereas when the human dental epithelium was recombined with the mouse dental mesenchyme, the growth rate of chimeric teeth did not obeys that of the human dental epithelium but that of the mouse dental mesenchyme, and thereby achieved an compact-size tooth equivalent to the size of mouse homogenous (mde+mdm) teeth after grown for 30 days (Fig. 1h, l). Immunostaining of the expression of two ameloblastic differentiation markers, Ameloblastin and MMP20, further confirmed the development phase alteration of the dental epithelium induced by heterogeneous dental mesenchyme. The expression of these two markers in the mouse dental epithelium-derived pre-ameloblasts in mde+hdm chimeric recombinants was delayed to 4th week after subrenal culture (Fig. 1m-o), whereas the expression of the two markers was antedated at 9-day in the human dental epithelium-derived ameloblasts in hde+mdm chimeric recombinants in subrenal culture (Fig. 1s-u), which is similar to the expression of them at 7-day in the ameloblasts derived from mouse dental epithelium in mde+mdm control recombinants (Fig. 1p-r). The possibility of tissue contamination was ruled out using specific primary antibodies against mouse or human MHC I antigens to distinguish between human and mouse tissues in the heterogonous chimeras (Fig. S1). Our results unambiguously indicate that dental mesenchyme is a crucial component that dominates the tooth growth rate and size by interaction with dental epithelium via diffusible signals during odontogenesis.

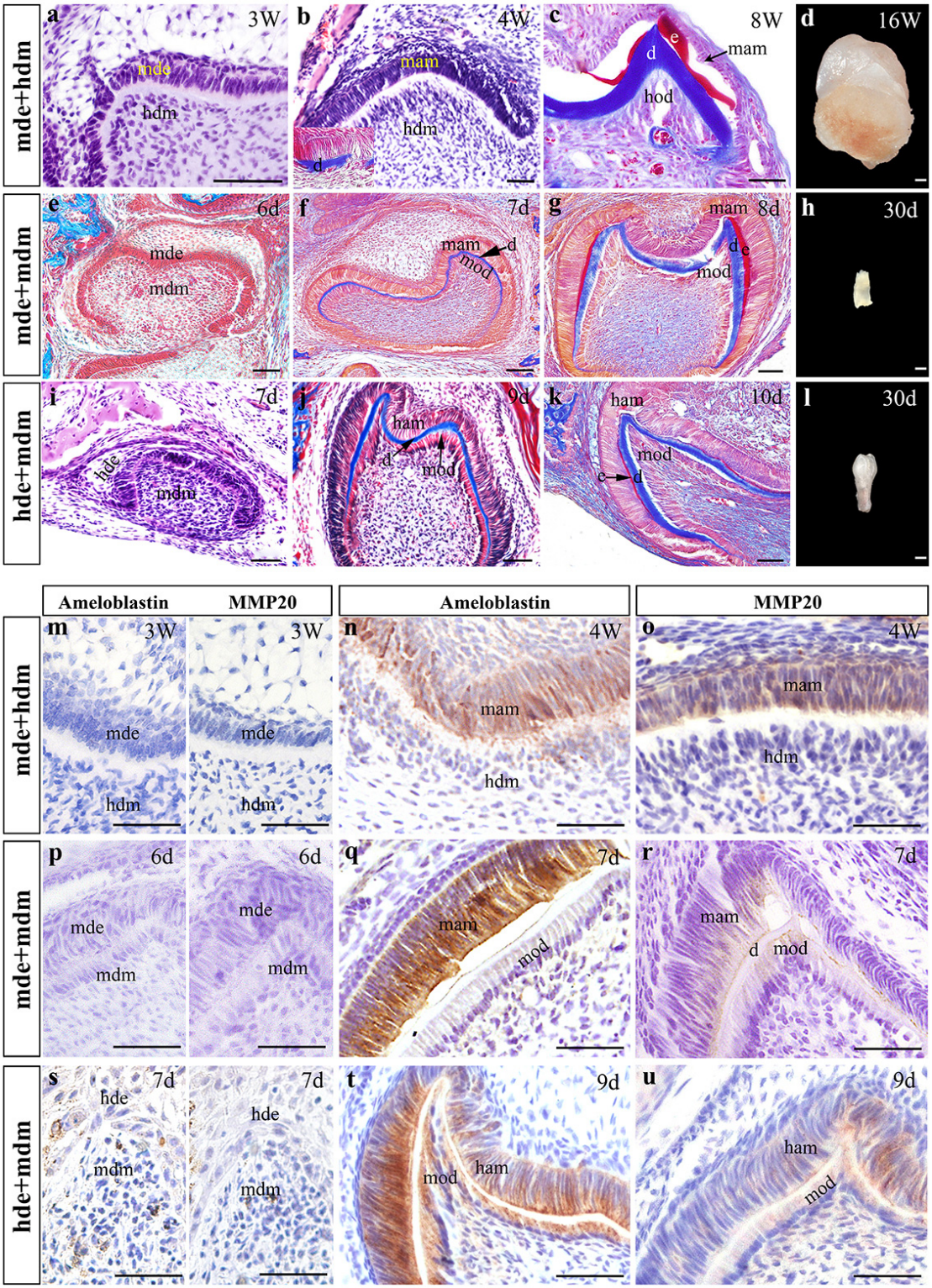

Fig. 1 Heterogeneous recombination of human and mouse dental tissues reveal the dominant role of the dental mesenchyme in control of the tooth growth in humans and mice. a-d Recombinants of E13.5 mouse dental epithelium and human bell-stage dental mesenchyme were cultured in kidney capsule for 3 weeks (**a**), 4 weeks (**b**), 8 weeks (**c**), and 16 weeks (**d**, whole mount). **e-h** Recombinants of E13.5 mouse dental epithelium and E13.5 mouse dental mesenchyme were

cultured in kidney capsule for 6 days (**e**), 7 days (**f**), 8 days (**g**), and 30 days (**h**, whole mount). **i-l** Recombinants of human bell-stage dental epithelium and E13.5 mouse dental mesenchyme were cultured in kidney capsule for 7 days (**i**), 9 days (**j**), 10 days (**k**), and 30 days (**l**, whole mount). **m-u** The expression of Ameloblastin and MMP20 in recombinants of E13.5 mouse dental epithelium and human bell-stage dental mesenchyme cultured in kidney capsule for 3 weeks (**m**), 4 weeks (**n** and **o**); recombinants of E13.5 mouse dental epithelium and mouse dental mesenchyme for 6 days (**p**), 7 days (**q** and **r**); recombinants of human bell-stage dental epithelium and mouse dental mesenchyme for 7 days (**s**) and 9 days (**t** and **u**). hdm, human dental mesenchyme; hde, human dental epithelium; mdm, mouse dental mesenchyme; mde, mouse dental epithelium; hod, human odontoblasts; mod, mouse odontoblasts; mam, mouse ameloblasts; d, dentin; e, enamel. Scale bar: a-c, e-g, i-k, and m-u = 50 μm, d, h, and l = 500 μm.

Table. 1 Ratio of tooth formation in different types of tissue recombinants.

Type of Recombinant		No. of Recombinant	No. of Tooth Formation	Ratio (%)
Epithelium	Mesenchyme			
mde	mdm	28	28	100
mde	hdm	78	76	97.4
hde	mdm	27	24	88.9

Abbreviations: mdm, E13.5 mouse dental mesenchyme; hdm, human bell-stage dental mesenchyme (14-16 weeks of gestation); mde, E13.5 mouse dental epithelium; hde, human bell-stage dental epithelium (14-16 weeks of gestation).

FGF signaling participates in the regulation of the tooth growth rate.

We next tried to figure out which signaling molecules might be involved in the regulation of tooth growth rate in humans and mice. Despite the fact that Hippo pathway is currently the only recognized signaling pathway in the control of the size and growth rate for several organs such as liver, knockout or overexpression experiments do not demonstrate its function in the supervision of growth rate and size

during tooth development [7, 21]. Conserved SHH, FGF, BMP, and Wnt pathways are all crucial signaling engaged in cell proliferation, apoptosis and differentiation during odontogenesis, indicating that they may be key players in orchestrating the fundamental mainspring of organ growth. Since the dental mesenchyme is dominant in the regulation of tooth growth (Fig. 1), we exclude epithelially expressed SHH signal [34]. To test whether mesenchymal BMP, FGF and WNT signaling may be involved in the regulation of tooth growth rate and size, we examined the level of the active indicators of these pathway including pSmad1/5/8 for BMP, K-Ras for FGF, and β-catenin for Wnt, respectively, in the chimeric tooth germs. The expression level of K-Ras in both dental epithelium and mesenchyme is much higher in the mde+hdm chimeric tooth germ (Fig. 2e), where the development of mouse dental epithelium-derived ameloblasts were dramatically delayed and remained immature after subrenal culture for 4 weeks, than that in the mouse homogenous recombinant tooth germ (Fig. 2b). By contrast, the expression levels of pSmad1/5/8 and β-catenin did not display apparent difference as compared between the heterogeneous recombinants and homogenous ones (Fig. 2a, c, d, f). Notably, there was an outstandingly enhanced activity of K-Ras in the mouse dental epithelium-derived ameloblasts of heterogeneous tooth germs but not in that of homogeneous recombinant controls (Fig. 2b, e). This enhanced epithelial FGF activity was certainly induced by human dental mesenchyme and may attribute to the protracted differentiation of mouse dental epithelium.

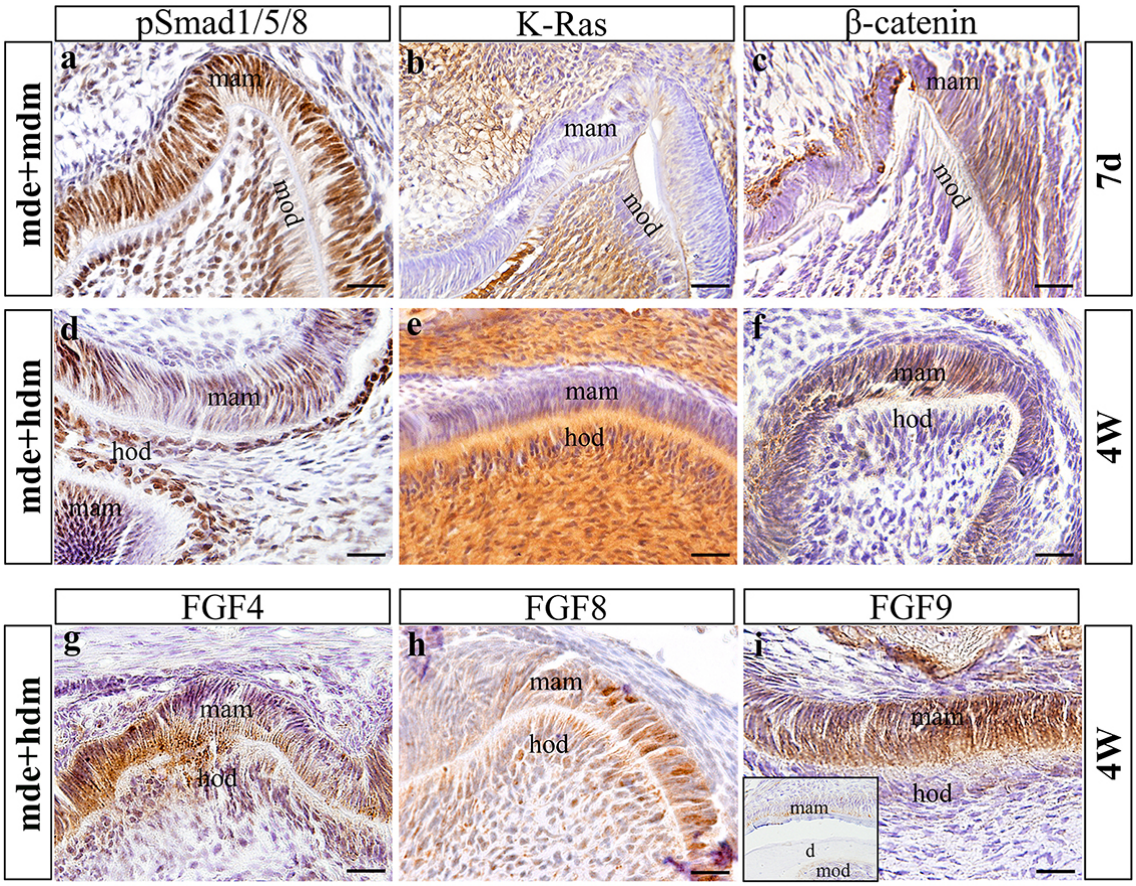

Fig. 2 FGF signaling in mouse dental epithelium is enhanced and reactivated when recombined with human dental mesenchyme. a-c The expression of pSmad1/5/8 (**a**), K-Ras (**b**), and β-catenin (**c**) in recombinants of mouse dental epithelium and mouse dental mesenchyme after 7-day subrenal culture. **d-f** The expression of pSmad1/5/8 (**d**), K-Ras (**e**), and β-catenin (**f**) in recombinants of mouse dental epithelium and human dental mesenchyme after 4-week subrenal culture. **g-i** The expression of FGF4 (**g**), FGF8 (**h**), and FGF9 (**i**, insert: not expressed in E18.5 mouse tooth germ) in recombinants of mouse dental epithelium and human dental mesenchyme after 4-week subrenal culture. mam, mouse ameloblasts; mod, mouse odontoblasts; hod, human odontoblasts. Scale bar = 25 μm.

To explore whether the upregulated FGF signaling may be associated with the prolonged tooth development phase and large tooth size in humans, we firstly searched for candidate FGFs that are persistently expressed in human developing dental mesenchyme but barely in mouse one. The most expression patterns of 22 known FGF

ligands in mammals have been verified in mouse tooth germs at the cap and bell stage (summarized in Table S1)[35, 36]. Our previous study had examined the expression patterns of *FGF3, FGF4, FGF7, FGF8, FGF9,* and *FGF10* in human tooth germs at different stages using *in situ* hybridization or immunohistochemistry [37]. Here, we screened the expression of the other 12 *FGFs* that have not been identified in human tooth germs by RT-PCR with exclusion of *FGF11, FGF12, FGF13,* and *FGF14* since they are not secreting ligands and do not activate FGF receptors as well. We found that, among them, *FGF1*, *FGF2*, *FGF15/19*, and *FGF18* were detectable at both the cap and the bell stage (data not shown). We further confirmed their expression in developing human teeth by section *in situ* hybridization (Fig. S2). Comparison of FGF expression data between human [37] and mouse [35, 36], we noticed that the majority of FGF transcripts are broadly distributed in the whole tooth germ including dental epithelium and mesenchyme throughout the early cap stage to the late bell stage in humans [37]. However, their expression is restricted to the limited region of tooth germs, such as enamel knot, and expressed in limited period of time in mice (Table. S1)[35, 36]. We believe this widely and persistently distributing pattern of FGF ligands in human tooth germs is closely related to their characteristics of tooth growth.

Further analysis of FGF expression data in humans and mice, we identified that FGF4, FGF8, and FGF9 ligands exhibit most distinctive patterns (Table. S1). These three ligands are persistently expressed in the dental epithelium and mesenchyme at least until the differentiation stage in humans [37]. However, in mice, they are either not expressed in the tooth germ or restricted in the enamel knot. Among them, what stands

out is FGF8. In mice, FGF8, being expressed in the dental epithelium at the laminar and early bud stage and no longer expressed at the late bud stage after E12 [38], has been demonstrated to play pivotal roles in early mouse tooth development, responsible for the determination of tooth forming sites and initiation of tooth development [35]. Whereas, in humans, *FGF8* transcripts is widely and intensively present in the whole tooth germ at least from the early cap stage to the differentiation stage [37]. Importantly, we found retained expression of FGF4, FGF9, and especially FGF8, in mouse dental epithelium derived pre-ameloblasts in mde+hdm recombinants after 4 week subrenal culture, where the development of mouse ameloblasts was largely delayed (Fig. 2g-i). Our results suggest that FGF signaling may play important roles and FGF8 could be a critical factor in the regulation of tooth growth rate and size.

Forced activation of *Fgf8* in mouse dental mesenchyme delays tooth growth and enlarges tooth size.

To validate whether *Fgf8* activity would regulate the tooth growth, we *ex vivo* overexpressed *Fgf8* in E13.5 molar mesenchyme using lentivirus, and cultivated the recombinant tooth germs in subrenal culture for designated days. Histological examination revealed that it took up to 9 days for *Fgf8*-overexpressed tooth grafts to start dentin secreting (Fig. 3b), whereas it only took 7 days for control ones to do so (Fig. 3a). Moreover, Ki67 staining detected remarkably higher level of proliferation rate in both the dental epithelium and mesenchyme of *Fgf8*-overexpressed tooth grafts compared to the controls after subrenal culture for 7 days (Fig. 3c-e; n = 6/group).

These data indicate that activated mesenchymal *Fgf8* activity delays tooth growth and dramatically stimulates the rate of cell proliferation.

To corroborate the aforementioned *ex vivo* results, we further generated *Wnt1-Cre;Rosa-Fgf8* transgenic mice to verify whether forced activation of mesenchymal *Fgf8* activity delays the tooth growth *in vivo*. Specifically dental mesenchymal overexpressed *Fgf8* was confirmed by anti-FGF8 immunostaining (Fig. S3). *Wnt1-Cre;Rosa-Fgf8* mice die of embryonic lethality beyond E15.0. Although histological examination revealed severe craniofacial hypoplasia in 100% cases, including exencephaly and the absence of identifiable tissues such as ears, auricles, eyes, nose, as well as tongue (data not shown), the mutant mice still possessed a pair of intact maxillary and mandibular molar germs (Fig. 4). More importantly, both the maxillary and mandibular molar germ exhibited an obvious retardation of tooth growth (Fig. 4). Since the mutant embryos die beyond E15.0, we grafted mutant molar germs in the subrenal capsule for further growing. As expected, the mutant teeth were grown with approximate one-day's delay when compared to the wild-type ones (Fig. 5a-f). Examination of the expression of odontoblast marker DSP and ameloblast marker Ameloblastin in the grafted teeth further confirmed this delay (Fig. 5i-l).

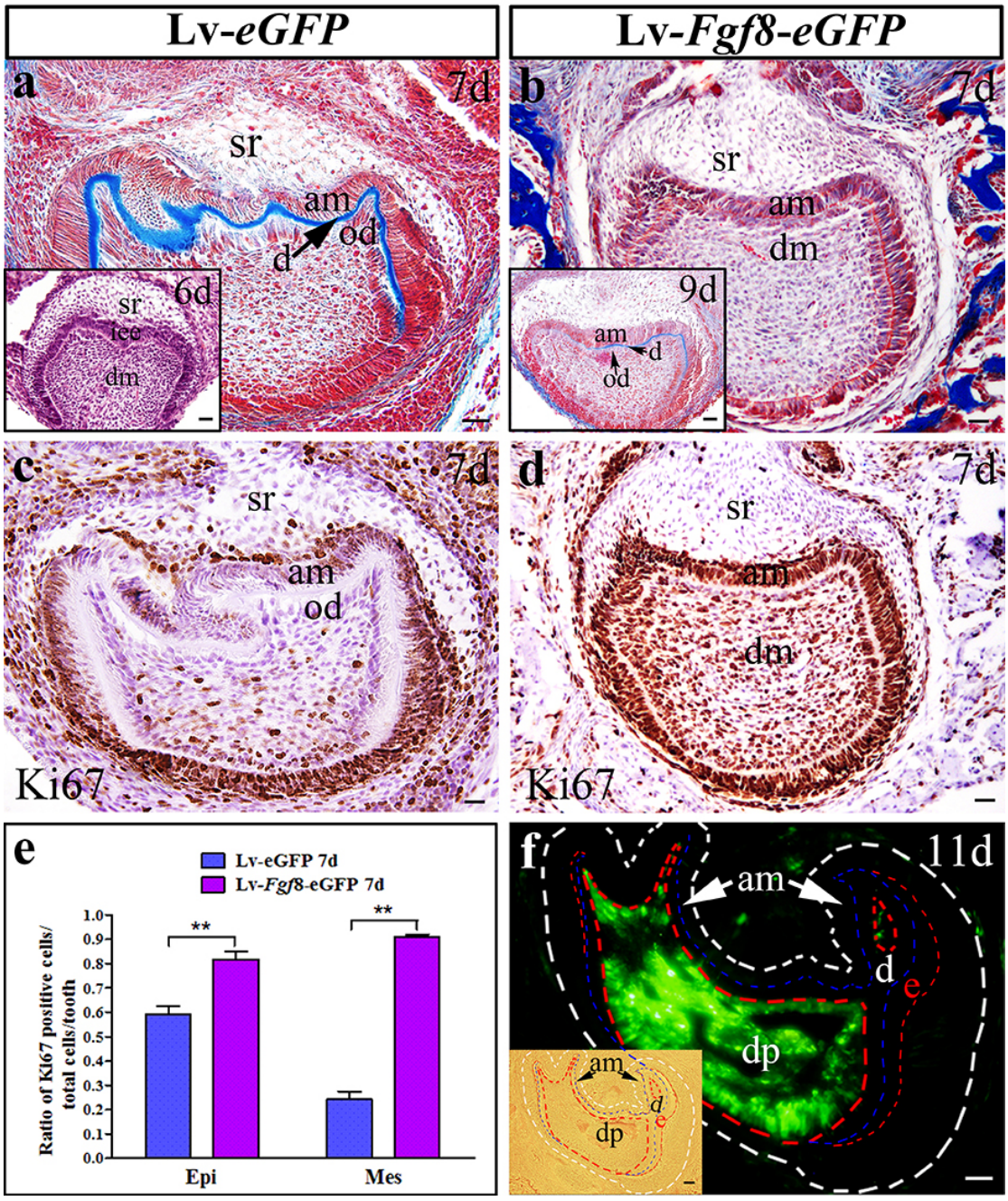

Fig. 3 Augmented *Fgf8* signaling in mouse dental mesenchyme delays tooth growth and increases cell proliferation. a, **b** Recombinants of E13.5 mouse dental epithelium and aggregates of dental mesenchymal cells infected with control LV-*eGFP* (**a**) or LV-*Fgf8-eGFP* (**b**) were cultured in the kidney capsule for 6 days (insert in **a**), 7 days, and 9 days (insert in **b**). **c**, **d** The expression of Ki67 in recombinants of E13.5 mouse dental epithelium and aggregates of dental mesenchymal cell infected with control LV-*eGFP* (**c**) or LV-*Fgf8-eGFP* (**d**), cultured in the kidney capsule for 7 days. **e** Comparison of Ki67-positive cells in the dental mesenchyme and dental epithelium of the recombinants. Standard deviation values were shown as error bars, and ** indicates $p<0.01$, n =

6/group. **f** GFP staining of recombinants of E13.5 mouse dental epithelium and aggregates of dental mesenchymal cell infected with control LV-*eGFP* cultured in the kidney capsule for 11 days. dm, dental mesenchyme; dp, dental pulp; am, ameloblasts; sr, stellate reticulum; od, odontoblasts; d, dentin; Epi, epithelium; Mes, mesenchyme. Scale bar = 50 μm.

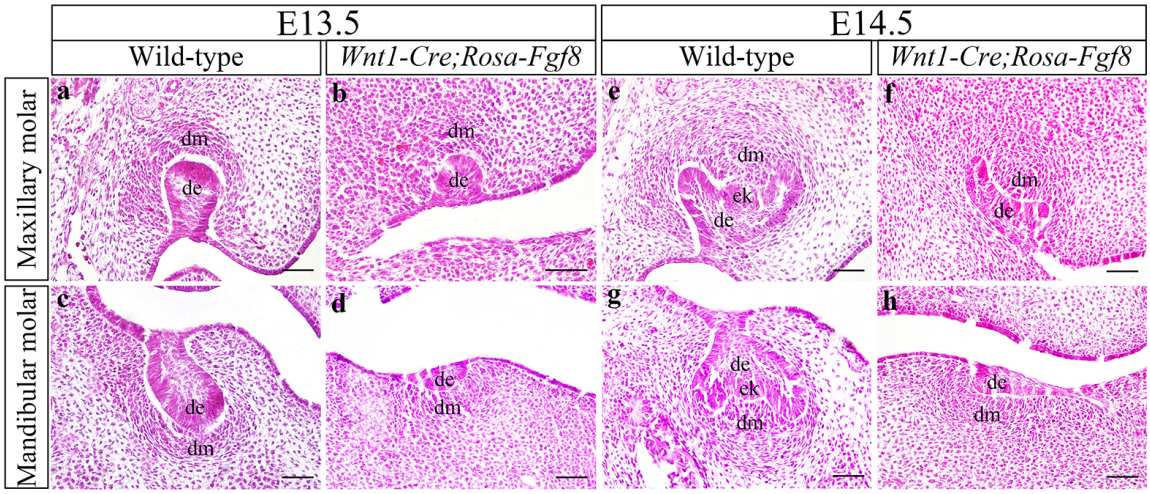

Fig. 4 *Wnt1-Cre;Rosa-Fgf8* mice exhibit delayed tooth growth during early tooth development. **a-d** Morphology of maxillary and mandibular molar in E13.5 wild-type (**a**, **c**) and mutant (**b**, **d**) mice. **e-h** Morphology of maxillary and mandibular molar in E14.5 wild-type (**e**, **g**) and mutant (**f**, **h**) mice. de, dental epithelium; dm, dental mesenchyme. Scale bar = 50 μm.

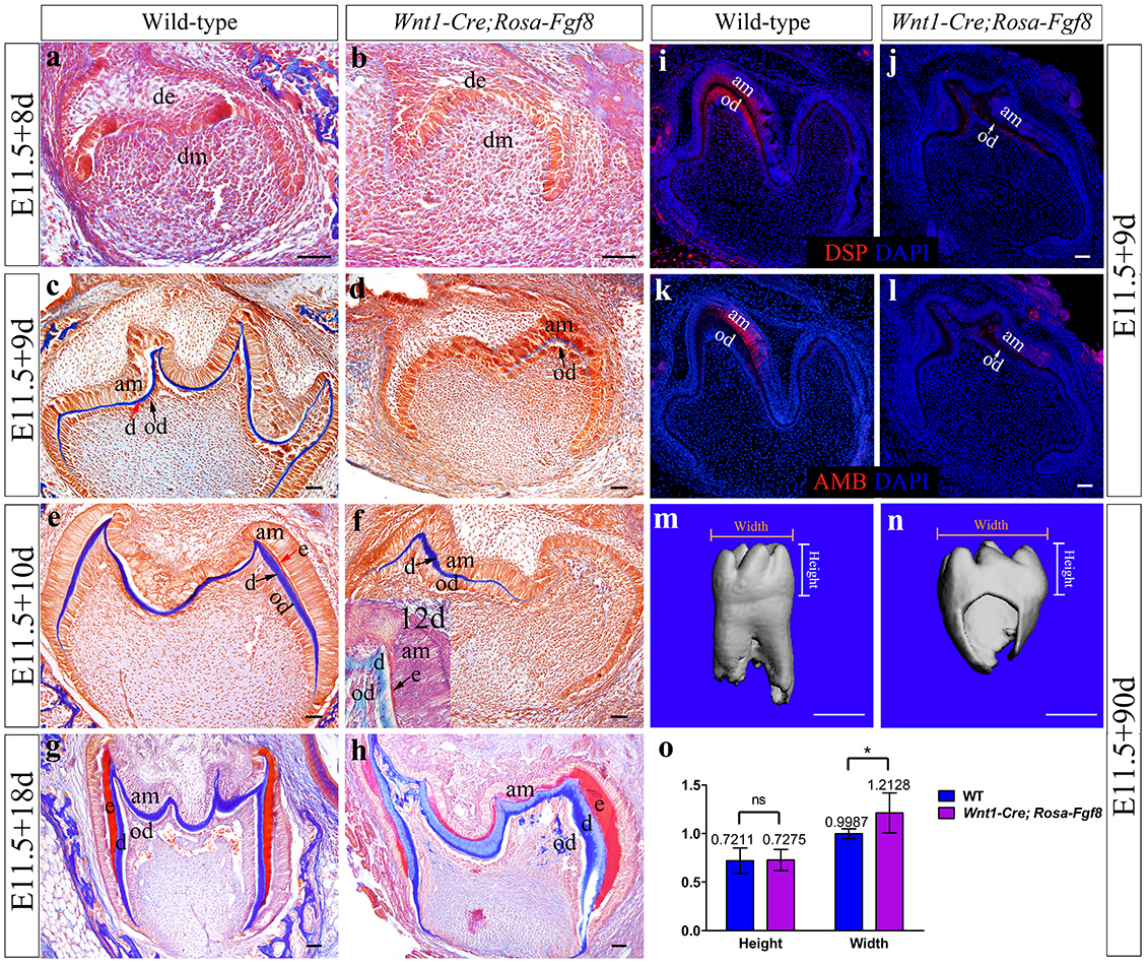

Fig. 5 ***Wnt1-Cre;Rosa-Fgf8*** **molar germs grafted in subrenal culture exhibit delayed tooth growth and enlarged tooth size. a-h** E11.5 wild-type and mutant molar germs were cultured in kidney capsule for 8 days (**a**, **b**), 9 days (**c**, **d**), 10 days (**e**, **f**), and 18 days (**g**, **h**). **i-l** The expression of DSP (**i, j**) and Ameloblastin (**k, l**) in E11.5 wild-type and mutant molar grafts after subrenal culture for 9 days. **m**, **n** Representative Micro-CT images of E11.5 wild-type (**m**) and mutant molar germs (**n**) after subrenal culture for 3 months. **o** Comparison of the height and width of the tooth crown between mutant and wild-type mineralized teeth after subrenal culture for 3 months. Standard deviation values were shown as error bars. ns indicates $p > 0.05$, and ** indicates $p < 0.01$, $n = 7$ and 11/group in **o**. de, dental epithelium; dm, dental mesenchyme; am, ameloblasts; od, odontoblasts; d, dentin; e, enamel. Scale bar: a-h, i-l = 50 μm; m and n = 500 μm.

Interestingly, the mutant graft teeth gained a larger size than the wild-type ones after 18 days in subrenal culture (Fig. 5g-h). To precisely evaluate the effect of mesenchymal *Fgf8* in the regulation of tooth size, grafts were cultured in the subrenal capsule for 3 months, allowing teeth for complete mineralization. Micro-CT was utilized to measure the height and width of the tooth crown in mutants and wild-types. Compared to wild-types (n = 7), although the height of the tooth crown in mutants (n = 11) has no difference, the width of the crown exhibited about 21% longer (Fig. 5m-o). Apparently, higher rate of cell proliferation contributes greatly to the larger teeth, which was evidenced by much more Ki67 positive cells presented in the grafted teeth of *Wnt1-Cre;Rosa-Fgf8* mice than that of wild-type controls (Fig. 6a-f, k-m, n = 3/group). Meanwhile, although an apoptotic marker Caspase3 staining was present in the layer of ameloblasts and odontoblasts in both mutant and wild-type tooth germs, apoptotic signal was non-detectable in pulp cells of mutant tooth germs, whereas it was detected in wild-type ones after 18 days in subrenal culture (Fig. 6g-j). These results further support the idea that ectopically activated Fgf8 signaling in mouse dental mesenchyme stimulates cell proliferation and prevents cell apoptosis during odontogenesis.

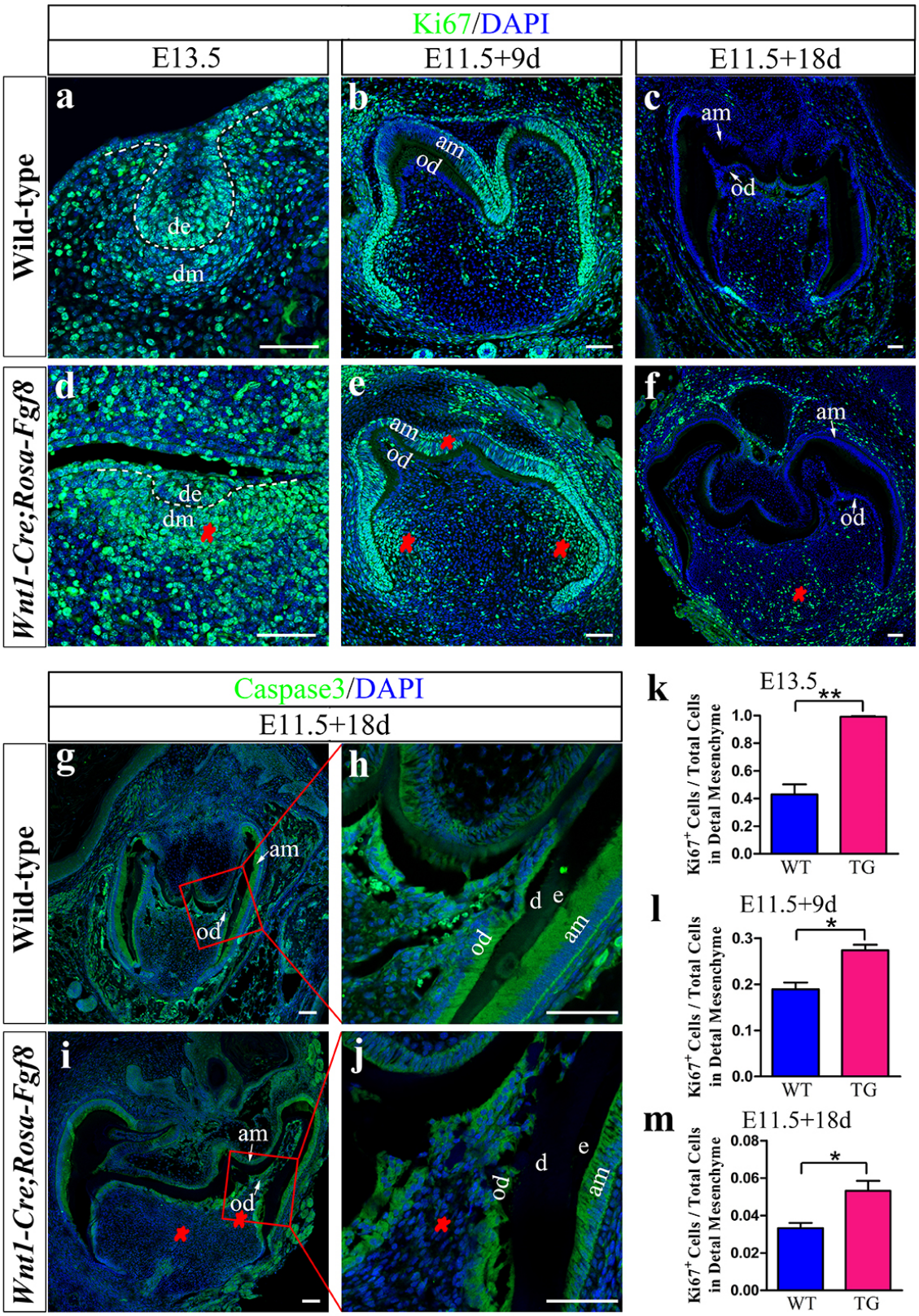

Fig. 6 Ectopically activated *Fgf8* signaling in mouse dental mesenchyme stimulates cell proliferation and prevents cell apoptosis during odontogenesis. a-f Immunostaining of Ki67 positive cells in E13.5 wild-type (**a**) and mutant (**d**) molar germs and in E11.5 wild-type and mutant molar germ grafts after subrenal culture for 9 days (**b**, **e**) and 18 days (**c**, **f**). **g-j** The expression of

Caspase3 in E11.5 wild-type (**g**, boxed area is magnified in **h**) and mutant (**I**, boxed area is magnified in **j**) molar germs after subrenal culture for 18 days. Note the absence of Caspase3 expression in the dental mesenchyme (red asterisk) excepting odontoblasts in mutant tooth grafts. **k-m** The percentage of Ki67 positive cells in the dental mesenchyme of wild-type and mutant E13.5 tooth germs (**k**) and tooth grafts after subrenal culture for 9 days (**l**) and 18 days (**m**), $n = 3$/group, * indicates $p < 0.05$. Standard deviation values were shown as error bars. am, ameloblasts; od, odontoblasts; d, dentin; e, enamel. Scale bar = 100 μm.

Ectopically activated dental mesenchymal FGF8 signaling is transduced via p38 and PI3K-Akt intracellular pathways.

To determine which intracellular pathway is implicated in the signal transduction of ectopically activated dental mesenchymal *Fgf8* signal, we detected the level of phosphorylated Erk1/2, P38, JNK, and PI3K-Akt, the activity indicators of MAPK pathway, in both E13.5 tooth germs and E11.5 ones cultured for 9 days in the kidney capsule. As shown in Fig. 7, no signal intensity difference in pErk1/2 (Fig. 7a-d) and pJNK (Fig. 7e-h) staining were observed between wild-type and mutant mice. Whereas, p38 signaling is dramatically elevated in *Wnt1-Cre;Rosa-Fgf8* teeth with a considerably increased amount of nuclear-localized pP38 cells both in the dental epithelium and dental mesenchyme of mutant E13.5 tooth germs and grafted teeth compared to the controls (Fig. 7i-l). Meanwhile, the intensity of PI3K-Akt staining was enhanced to some extent and the amount of pAkt1^{+} cells was increased in mutant E13.5 tooth germs (Fig. 7m, n) and grafted teeth (Fig. 7o, p). Western blot results further confirmed the increased expression of pP38 and pAkt1 in E13.5 mutant tooth germs (Fig. 7q, r; $n = 3$). Our results indicate that augmented dental mesenchymal *Fgf8* activity enhances P38

and PI3K-Akt signaling both in the dental mesenchyme and in the dental epithelium, suggesting that they may function as intracellular pathway for transducing FGF8 signals into nuclei.

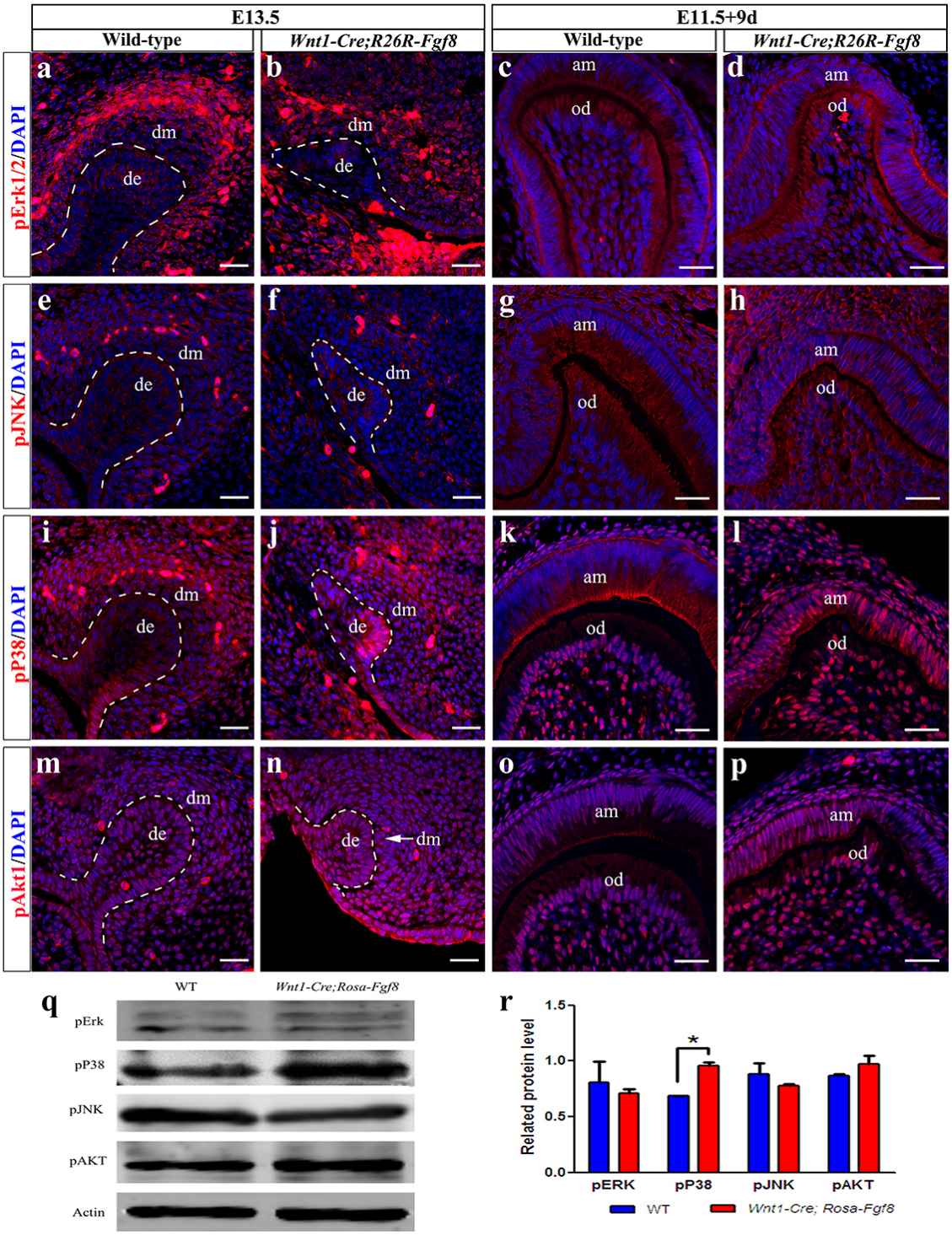

Fig. 7 Ectopically activated dental mesenchymal *Fgf8* signaling is transduced via p38 and PI3K-Akt intracellular pathways. a-d The expression of pErk1/2 in E13.5 wild-type (**a**) and

mutant (**b**) molar germs and in E11.5 wild-type (**c**) and mutant (**d**) molar germs after subrenal culture for 9 days. **e-h** The expression of pJNK in E13.5 wild-types (**e**) and mutants (**f**) molar germs and in E11.5 wild-type (**g**) and mutant (**h**) molar germs after subrenal culture for 9 days. **i-l** The expression of pP38 in E13.5 wild-type (**i**) and mutant (**j**) molar germs and in E11.5 wild-type (**k**) and mutant (**l**) after subrenal culture for 9 days. **m-p** The expression of pAkt1 in E13.5 wild-types (**m**) and mutants (**n**) molar germs and in E11.5 wild-type (**o**) and mutant (**p**) molar germs after subrenal culture for 9 days. **q** Western-blotting of pErk1/2, pP38, pJNK, and pAKT1 expressed in E13.5 wild-type and mutant molar germs. **r** Quantification of immunoblotting data in **q**. $n = 3$/group. * indicates $p < 0.05$. Standard deviation values were shown as error bars. de, dental epithelium; dm, dental mesenchyme; am, ameloblasts; od, odontoblasts. Scale bar = 25 μm.

Enhanced dental mesenchymal *Fgf8* activity promotes the transition of the cell cycle from G1- to S-stage during odontogenesis.

The rate of cell proliferation controlled by cell cycle progression [3] is a key player in organ size control and also closely associated with tissue differentiation status, as higher cell proliferation always presents in developing tissues and lower one in differentiated ones. Since the elevation of *Fgf8* in the dental mesenchyme results in the significant promotion of cell proliferation and prevention of cell apoptosis (Fig. 6), we speculated that enhanced dental mesenchymal FGF8 signaling would morph cell cycling. To verify this hypothesis, we set forth to ascertain the distribution of cyclin D1 (Ccnd1) and its inhibitor $p21^{Cip1}$ (p21), a pair of critical regulators to function stimulatory and repression effect for inducing cell cycle entry and thus to mediate the G1-S stage transition [39, 40], in E13.5 tooth germs and grafted teeth. As shown in Fig. 8, although the same high density of $Ccnd1^{+}$ cells were present in the dental epithelium of E13.5 wild-type and mutant tooth germs, the dental mesenchyme in mutant tooth germs

possessed an considerably increased amount of Ccnd1^{+} cells in comparison to that in wild-type ones (Fig. 8a, e). On the other hand, p21^{+} cells were abundantly present in presumptive primary enamel knot of the dental epithelium and slightly in the dental mesenchyme in wild-type mice but totally absent from the whole tooth germ in mutant ones (Fig. 8b, f). Thereout, more colocalization of Ccnd1 and p21 staining were found in the wild-type tooth germs than in the mutant ones (Fig. 8c-d, g-h). In grafted teeth, nuclear Ccnd1^{+} cells were distributed not only in ameloblasts and odontoblasts (Fig. 8m, p-up) but also all over the dental pulp in mutants (Fig. 8m, p-down), rather than being restricted to the dental mesenchymal cells adjacent to the odontoblasts in wild-types (Fig. 8i, l). Although p21 was expressed in ameloblasts and dental mesenchymal cells in both wild-type and mutant teeth, its expression level was relatively decreased in mutants (Fig. 8j, l, n, p). In addition, the nuclear localization of p21 could be detected in dental mesenchymal cells of wild-type teeth (Fig. 8l-down), whereas it was found to be in the cytoplasm of grafted mutant teeth (Fig. 8p-down), which make it unable to cooperate with nuclear Ccnd1 to regulate the cell cycle progression in the dental mesenchymal cells. Taken together, these results provide strong evidences that enhanced mesenchymal *Fgf8* activity observably elevates the activity of nuclear Ccnd1 while degrades the activity of nuclear p21, thus stimulation of Ccnd1 and repression of p21 both function to induce cell cycle entry and promote the transition of cell cycle from G1- to S- stage, which will facilitate cell population to retain the high rate of proliferation.

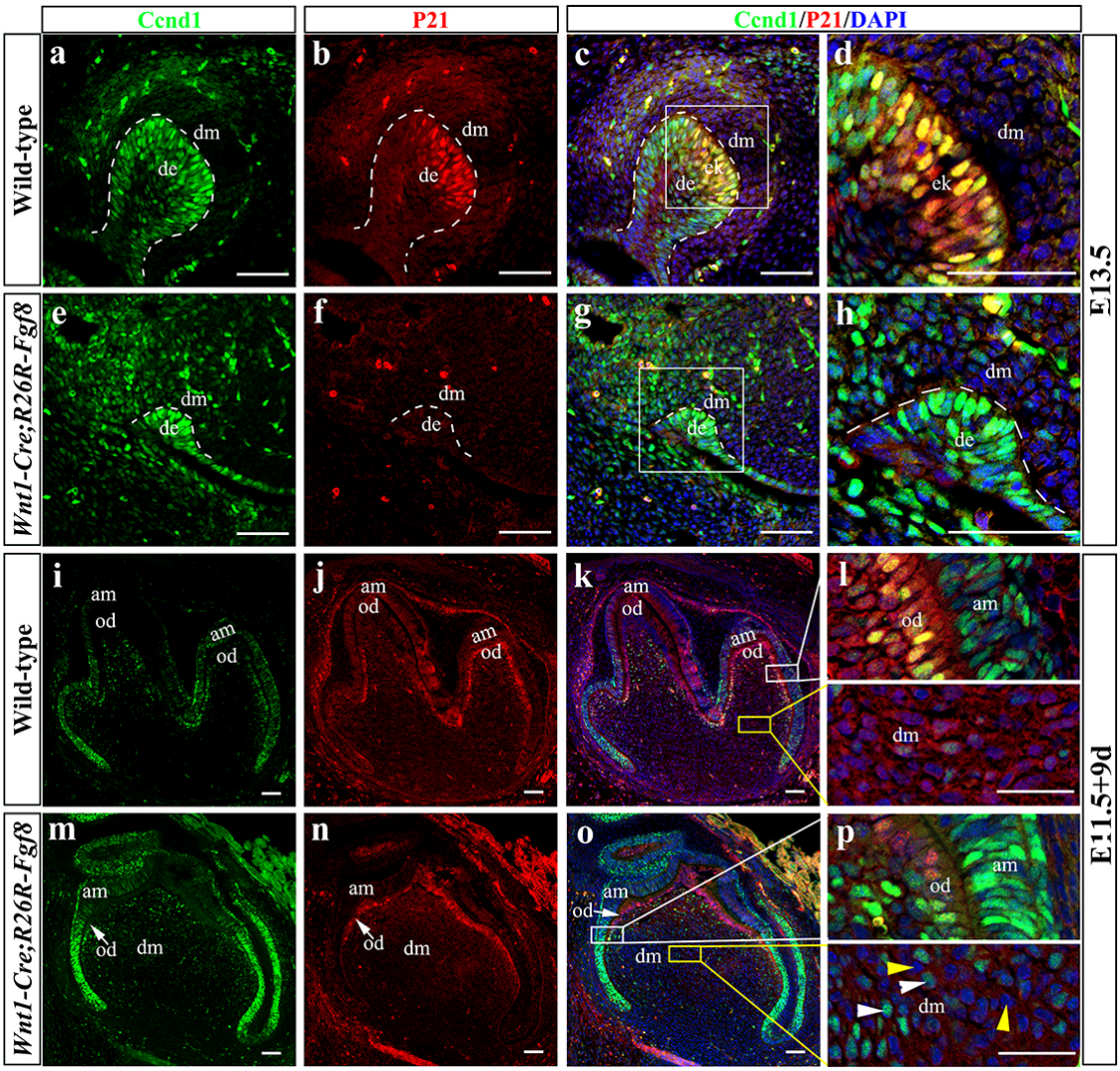

Fig. 8 Enhanced dental mesenchymal *Fgf8* activity increases the level of nuclear Ccnd1 and decreases the level of nuclear p21. The colocalization of Ccnd1 and P21 in E13.5 wild-type (**a-d**) and mutant (**e-h**) molar germs and E11.5 wild-type (**i-l**) and mutant (**m-p**) molar germs after subrenal culture for 9 days. White and yellow boxed areas in (**c**), (**g**), (**k**), and (**o**) are magnified in (**d**), (**h**), (**l**), and (**p**), respectively. Note the significantly increased proportion of Ccnd1-positive cells (white arrow) and the shift of P21 from the nuclei to the cytoplasm (yellow arrow) in mutant dental mesenchyme (**p**) as compared with wild-type ones (**l**). de, dental epithelium; dm, dental mesenchyme; am, ameloblasts; od, odontoblasts. Scale bar: a-n, p-s = 50 μm; o, t = 25 μm.

Discussion

The heterospecific recombination study carried out between the mouse and rat molar tooth germs has suggested that tooth size is determined by dental mesenchyme [41, 42]. Additionally, our recent studies showed that, in comparison with natural development phase, the differentiation duration of mouse dental epithelium or non-dental epithelium into ameloblasts when induced by human dental mesenchyme is significantly extended, whereas that of human dental epithelium or epithelial stem cells into ameloblasts when induced by mouse dental mesenchyme is significantly shortened [32, 33]. These results are consistent with growth rate difference between human and mouse teeth [14], suggesting a dominant role of the dental mesenchyme in regulation of tooth development rate. This idea is further supported by our current heterospecific recombination study carried out between the mouse and human molar tooth germs (Fig. 1). We further provide unambiguous evidences that not only the tooth size but also the tooth growth rate are obedient to hereditary character of the dental mesenchyme.

Hippo signaling is the only admitted signaling pathway that plays its best-known physiological function on organ size in the mouse model for mammalian lineage [6-9], which mainly involves in the regulation of cell proliferation and apoptosis and thereby cell number [10]. Activation or inhibition of YAP/TAZ, a transcriptional co-activator of Hippo pathway, leads to the adjustment of cell proliferation and apoptosis, thus affect organ sizes and tissue homeostasis [6-9]. However, in tooth development, suppression of YAP *ex vivo* at the cap stage only leads to ectopic cusp formation [21], while overexpression of YAP *in vivo* disrupts tooth morphogenesis with abnormal enamel

knot as well as greatly widened dental lamina; teeth ultimately formed in YAP transgenic mice do not exhibit any growth delay or size enlargement [7]. These data suggest that the renowned control function of Hippo pathway in mammalian organ size is not applicable for the tooth organ. In support of this notion, it has also been reported that size-control mechanisms differ across mammalian organs [4] and enhanced Hippo signaling induces organ enlargements in the stomach, heart, liver, and spleen, but not in lung, kidney, and intestine [11-13].

Conserved pathways, such as FGF, BMP, Hh, and WNT, participate in the highly conserved molecular mechanism underlying organismal growth by corresponding alterations of cell growth and division [3-5]. FGFs, as the most common mitogens, are positively correlated to the rate of cell growth and cell division and involved in the induction and pattern formation during tooth development [43, 44]. Fgf8 has been demonstrated to play an important role in cell survival and proliferation of CNC cells [45], and exerts a positive effect on proliferation of dental mesenchymal cells [38]. Our data show that FGF signaling rather than BMP and WNT signaling is highly active in human-mouse chimeric tooth germs where the development phase of mouse dental epithelium is largely slowed down (Fig. 2), which is consistent with the continuously high expression of FGFs, particularly FGF8, in human tooth germs, suggesting a potentially positive role of FGF signaling in regulating the tooth growth rate and size during odontogenesis in humans. Both our *ex vivo* lentivirus-mediated overexpression system and *in vivo* transgenic mouse model support that forcibly activated dental mesenchymal *Fgf8* activity stimulates cell proliferation and inhibits cell apoptosis, thus

prolongs tooth development rate and enlarges tooth size in mice (Fig. 3-6). We therefore believe that FGF8 is a critical intrinsic factors in regulating the tooth growth rate and size during mammalian odontogenesis.

Functional redundancy complicates interpretation of FGF genetic studies. Phenotypes in various *Fgfr* knockout mice have demonstrated that different FGF receptors have both essential and redundant roles throughout development [43]. During odontogenesis, FGF7 and FGF10 have been proven to act as surrogates of mesenchymal FGF3 [46], and FGF4, FGF8, as well as FGF9 have also been suggested functional redundancy and repetitive use in mouse tooth development [14]. Our previous and current study show that several FGFs, especially FGF4, FGF8, and FGF9, have a broad and persistent expression in the whole tooth germs in humans but are restricted to the limited region of tooth germs in mice [37] (Table. S1). These data suggest that tooth growth rate and size may be the product of synergistic effects of different FGFs in mammals. Actually, in addition to the fact that FGF8 is a key intrinsic factor to control tooth growth rate and size discovered in the current study, Fgf9 has also been reported to induce cell proliferation in cultured mouse dental mesenchyme *in vitro* [38] as well as in cervical loop development *in vivo* [47] and the *Fgf9* null mutant mice show a size-reduced labial cervical loop [47], and FGF4 stimulates cell proliferation in both dental epithelium and mesenchyme as well [38, 48], both suggesting their positive function on the regulation of tooth growth and size. We speculate that, in humans, many broadly, intensively, and persistently expressed FGF ligands may act in concert to confer growth capability (stimulation of proliferation and prevention of apoptosis) on tooth tissues to

achieve longer development phase and larger size.

Transduction of FGF signaling is mediated by multiple intracellular pathways, including P38, PI3K/Akt, Erk1/2, and JNK [43]. In our previous study, the similar expression patterns of the indicators in Erk, P38, JNK, and PI3K-Akt pathways in mouse and human tooth germs suggests their conservative regulatory functions during mammalian odontogenesis [37]. p38 MAPK has been reported to be involved in control of the cell cycle in mouse skeletal muscle cells [49], human dental pulp stem cells [50], and rat mesenchymal stem cells [51], which is also significantly increased in our *Wnt1-Cre;Rosa-Fgf8* mice (Fig. 7). The PI3K-Akt pathway is associated with a variety of cellular functions including cell growth, cell cycle regulation, and cell survival [52]. The increased PI3K-Akt level can regulate the proliferation and differentiation of auditory progenitors and neural progenitor cells by the activation of the cell cycle during organogenesis [53, 54]. Moreover, Akt protein is a central intracellular factor to transduce and integrate multiple extracellular growth factor signals, such as FGF, BMP, and GH/IGF, into a comprehensive signal network to supervise the processes of cell proliferation, growth, and survival [4]. The increased activity of PI3K-Akt pathway caused by augmented *Fgf8* in the cranial neural crest cell (Fig. 7) further supports its positive function in cell growth and cell cycle regulation. Erk has been reported to provide a switch-like transition between proliferation and differentiation of muscle progenitors [55], while JNK pathway has been elucidated to play crucial role in negative growth regulation and likely performs a central regulator in both local growth coordination and global growth coordination [3]. Both two pathways did not show any

noticeable alteration in our *Fgf8* transgenic mice, which may attribute to their main function in control of negative growth or balancing cell proliferation and differentiation.

Cell growth and division are controlled by the cyclin depend kinases (CDKs) and their binding partners (cyclins) that regulate cell cycle progression through the regulation of the G1-S and G2-M transition. Many cell cycle regulators have been proved to control organ growth and size, which appear to be generally conserved in *Drosophila* and mammals [(3)]. The G1-S phase transition is a rate-limiting step, a known checkpoint between cell growth and cell division, requiring cell cycle regulators to monitor and regulate the progression of the cell cycle [(56)]. The stimulatory effects of cyclins can be offset by CDKs inhibitors (CDKIs) and the repression of CDKIs is also a prerequisite for G1-S transition, only elevating the level of cyclin D1 is not sufficient to induce cell cycle entry [(57)]. Cyclin D1 (Ccnd1) is synthesized rapidly in the G1 phase and accumulates in the nucleus and degraded as the cell enters the S phase [(39)]. P21, known as CDKI1, functions as a regulator of cell cycle progression in G1 and S phase and inhibits all cyclin/CDK complexes, which in turn results in cell cycle arrest and/or apoptosis [(40)]. Enhanced dental mesenchymal *Fgf8* might promotes cell cycle progression through the regulation of the G1-S transition, which further stimulates cell proliferation and prevents cell differentiation and apoptosis, thereby resulting in prolonged tooth growth and larger tooth size. In line with this notion, we found that the amount of nuclear Ccnd1^{+} cells is dramatically increased while that of nuclear P21^{+} cells is markedly decreased in the dental mesenchyme at both the early and differentiation stage in *Wnt1-Cre; Rosa-Fgf8* mice as compared to those in the control

(Fig. 8), stating that forcedly enhanced *Fgf8* in the dental mesenchyme could elevates the level of Ccnd1 and meanwhile suppresses the level of p21. Stimulation of Ccnd1 and repression of p21 both constitute the prerequisites to induce cell cycle entry and thereby to promote the G1-S transition.

Tissue bioengineering based on the principle of Developmental Biology represents a promising approach for repair and regeneration of damaged tissues and organs in the future. However, unmatched development phase and organ size between humans and the model animals such as Drosophilae, Zebra fishes, and mice provide to be a major obstacle to acquire knowledge about organ growth control in humans. Uncovering of the molecular mechanism underlying organ growth control in humans is a prerequisite for the realization of replacement therapy in the future. Our study provides important FGF signaling information in tooth developmental process and enlightens our knowledge about the nature of FGF signaling in human tooth growth.

Materials and methods

Mouse models

Wnt1-Cre and *Rosa-Fgf8* mice were obtain from Jackson Laboratory [58]. Dental mesenchymal-specifically overexpressed *Fgf8* mice were generated by crossing *Wnt1-Cre* mice with *Rosa-Fgf8* mice. Mutant embryos were identified by PCR genotyping. All wild-type mice were on the CD-1 background.

Tissue recombination, organ culture, and subrenal culture

Fresh lower jaws isolated from human fetuses of 14th-16th week gestation following medical termination of pregnancy were provided by Maternal and Child Health Hospital of Fujian Province, China. The precise embryonic age of fetuses was defined by the measurement of the crown-rump length (CRL) [31]. Human and E13.5 mouse embryonic tooth germs were dissected out in ice-cold PBS and then treated with Dispase II for 20 min at 37℃. The dental mesenchyme and dental epithelium was separated with the aid of fine forceps and incubated on ice for further recombination experiments. Three types of tissue recombination were performed, including recombination of human bell-stage dental mesenchyme (14-16 weeks of gestation) that possesses odontogenic potential [31] with E13.5 mouse dental epithelium (referred to as mde+hdm); recombination of mouse E13.5 dental mesenchyme that possesses odontogenic potential with human bell-stage dental epithelium (hde+mdm); and recombination of E13.5 mouse dental mesenchyme with mouse dental epithelium at the same stage as control （mde+mdm）. All recombinants were further cultured in the Trowell-type organ culture dish overnight, followed by sub-renal grafting in adult nude

mice, as described previously [31, 59]. The use of animals and human tissues in this study was approved by the Ethics Committee of Fujian Normal University (permission #2011005).

Lentivirus infection and cell re-aggregation

For efficient infection of lentivirus [60], isolated E13.5 mouse dental mesenchyme was digested with 0.25% trypsin at 37 °C for 5 min and then gently pipetted 3-10 times to be dissociated into a single-cell suspension. To make a dental mesenchyme pellet, about 5×10^5 dental mesenchymal cells were infected with 20 μL concentrated lentivirus in 200 μL culture medium in an Eppendorf tube. The tube was incubated at 37℃ in a 5% CO_2 environment for 2 hours with its cap open, centrifuged at 3000 rpm for 3 min, and then incubated again in the same situation for 2 hours. Cell pellets were removed from the tubes, recombined with the E13.5 dental epithelium, and cultured in the Trowell-type organ culture dish overnight. Recombinants were subjected to sub-renal grafting and cultured in nude mice.

Histology, *in situ* hybridization, immunostaining, and Western blot

For histological analysis, harvested samples were fixed in 4% paraformaldehyde (PFA)/PBS, dehydrated, embedded in paraffin, and sectioned at 7 μm. Standard Hematoxylin/Eosin (H&E) and Azan dichromic staining were utilized for histological analysis [61]. Ossified tissues or grafts were demineralized with EDTA/PBS for a week prior to dehydration. For *in situ* hybridization, dental tissues from staged human embryos were dissected out in ice-cold PBS and fixed in 4% RNase-free PFA/PBS at 4°C overnight. Human cDNAs, including *FGF1* (MHS6278-202758608), *FGF2*

(EHS1001-208062206), *FGF15/19* (MHS6278-202756089), *FGF18* (MHS6278-202830446), were purchased from Open Biosystems (Alabama, USA) and were subcloned to pBluescript-KS plus vector for riboprobe transcription. Whole-mount *in situ* hybridization and section *in situ* hybridization were performed following a standard protocol as described previously [62, 63]. Immunostaining was performed as described previously [64]. The following primary antibodies were used including the products of Santa Cruz Biotechnology (Texas, USA): Ameloblastin, DSP, K-Ras, FGF8, P21; ABCam: Amelogenin, FGF4, FGF9, Caspase3, Ccnd1; Cell Signaling Tech (Massachusetts, USA): pSmad1/5/8, pP38, pErk1/2, pJNK, pAKT1; Merck Millipore: β-catenin; and Spring Bio: Ki67. Alexa Fluor 488 or 594 IgG (H+L) antibody (Thermo Fisher, Massachusetts, USA) and horseradish peroxidase-coupled IgG antibody (Santa Cruz) were used as the secondary antibody. For immunoblotting, pP38, pErk1/2, pJNK, pAkt, and Actin (Santa Cruz) were used as primary antibodies. IRDye 800cw or 680cw IgG (Odyssey, Nebraska, USA) were used as secondary antibodies. Immunoblotting was conducted as described previously [65]. Signals were observed using microscope (Olympus BX51, Tokyo, Japan), Laser scanning confocal microscope (Zeiss LSM780, Jena, Germany), and Infrared Imaging Systems (Odyssey C1x). Representative images were taken from a minimum of 3 replicate experiments.

Micro-computed tomography imaging and analysis

Harvested mineralized teeth were scanned with X-ray micro-computed tomography (microCT) equipment (μCT50, SCANCO Medical AG, Fabrikweg2, CH-8306 Bruettisellen, Switzerland). The microCT parameters were as follows: 19 × 19

mm–field of view, 15-μm voxel size, 70 kVp, 200 mA, 360° rotation, 1500ms exposure time. All datasets were exported in the DICOM format with the isotropic 15-μm^3 voxel. Acquired height and width of the tooth crown were analyzed with the attached software of μCT50.

Statistics analysis

Image J software (version 1.46r; National Institutes of Health, USA) was utilized for Ki67-positive cell counting and to detect the densitometry of the western blot bands with at least three biological replicates counted. Statistical analyses were performed with GraphPad Prism 5 (Version 5.01; GraphPad Software Inc, California, USA). Data were represented as mean ± SD. Paired *t*-test was used to evaluate differences between two groups, and analysis of variance (ANOVA) was used to determine differences among different groups. If there was a significance of ANOVA test, Bonferroni's posthoc test was used. p values <0.05 is considered statistically significant difference.

Acknowledgments

This study was supported by the National Natural Science Foundation of China (81870739, 81271102, 81771034) and the Natural Science Foundation of Fujian Province (2019J01281).

Competing interests

The authors declare no competing interests.

References

1. Promislow DEL, Harvey PH. Living fast and dying young: A comparative analysis of life‐history variation among mammals. Proceedings of the Zoological Society of London. 1990;220(3):417-37.
2. Swanson EM, Dantzer B. Insulin-like growth factor-1 is associated with life-history variation across Mammalia. Proc Biol Sci. 2014;281(1782):20132458.
3. Gokhale RH, Shingleton AW. Size control: the developmental physiology of body and organ size regulation. Wiley Interdiscip Rev Dev Biol. 2015;4(4):335-56.
4. Penzo-Mendez AI, Stanger BZ. Organ-Size Regulation in Mammals. Cold Spring Harb Perspect Biol. 2015;7(9):a019240.
5. Lui JC, Garrison P, Baron J. Regulation of body growth. Curr Opin Pediatr 3 (2744). 2015;27(4):502-10.
6. Barry ER, Morikawa T, Butler BL, Shrestha K, de la Rosa R, Yan KS, et al. Restriction of intestinal stem cell expansion and the regenerative response by YAP. Nature 1 (42351). 2013;493(7430):106-10.
7. Liu M, Zhao S, Wang XP. YAP overexpression affects tooth morphogenesis and enamel knot patterning. J Dent Res 2 (4144). 2014;93(5):469-74.
8. Yu FX, Zhao B, Guan KL. Hippo Pathway in Organ Size Control, Tissue Homeostasis, and Cancer. Cell 1 (33116). 2015;163(4):811-28.
9. Zhang P, Pei C, Wang X, Xiang J, Sun BF, Cheng Y, et al. A Balance of Yki/Sd Activator and E2F1/Sd Repressor Complexes Controls Cell Survival and Affects Organ Size. Dev Cell 1 (10366). 2017;43(5):603-17 e5.
10. Tumaneng K, Russell RC, Guan KL. Organ size control by Hippo and TOR pathways. Curr Biol 1 (9916). 2012;22(9):R368-79.
11. Song H, Mak KK, Topol L, Yun K, Hu J, Garrett L, et al. Mammalian Mst1 and Mst2 kinases play essential roles in organ size control and tumor suppression. Proc Natl Acad Sci U S A. 2010;107(4):1431-6.
12. Heallen T, Zhang M, Wang J, Bonilla-Claudio M, Klysik E, Johnson RL, et al. Hippo pathway inhibits Wnt signaling to restrain cardiomyocyte proliferation and heart size. Science 1 (31477). 2011;332(6028):458-61.
13. Dong J, Feldmann G, Huang J, Wu S, Zhang N, Comerford SA, et al. Elucidation of a universal size-control mechanism in Drosophila and mammals. Cell 1 (33116). 2007;130(6):1120-33.
14. Zhang YD, Chen Z, Song YQ, Liu C, Chen YP. Making a tooth: growth factors, transcription factors, and stem cells. Cell Res 1 (11981). 2005;15(5):301-16.
15. Polly PD. Gene networks, occlusal clocks, and functional patches: new understanding of pattern and process in the evolution of the dentition. Odontology 4 (1354). 2015;103(2):117-25.
16. Jheon AH, Seidel K, Biehs B, Klein OD. From molecules to mastication: the development and evolution of teeth. Wiley Interdiscip Rev Dev Biol. 2013;2(2):165-82.
17. Salazar-Ciudad I. Tooth patterning and evolution. Curr Opin Genet Dev 2 (8568). 2012;22(6):585-92.
18. Schoenwolf GC BS, Brauer PR, Francis-West PH. Larsen's Human Embryology E-Book. 2014.
19. Rodrigues HG, Renaud S, Charles C, Le Poul Y, Sole F, Aguilar JP, et al. Roles of dental

development and adaptation in rodent evolution. Nat Commun (10742). 2013;4:2504.
20. Line SR. Variation of tooth number in mammalian dentition: connecting genetics, development, and evolution. Evol Dev 3 (2684). 2003;5(3):295-304.
21. Kwon HJ, Li L, Jung HS. Hippo pathway/Yap regulates primary enamel knot and dental cusp patterning in tooth morphogenesis. Cell Tissue Res 3 (3333). 2015;362(2):447-51.
22. Edelman GM. Morphoregulation. Dev Dyn. 1992;193(1):2-10.
23. Thesleff I, Sharpe P. Signalling networks regulating dental development. Mech Dev. 1997;67(2):111-23.
24. Jernvall J, Thesleff I. Reiterative signaling and patterning during mammalian tooth morphogenesis. Mech Dev. 2000;92(1):19-29.
25. Lloyd AC. The regulation of cell size. Cell 1 (33116). 2013;154(6):1194-205.
26. Tummers M, Thesleff I. The importance of signal pathway modulation in all aspects of tooth development. J Exp Zool B Mol Dev Evol. 2009;312B(4):309-19.
27. Plikus MV, Zeichner-David M, Mayer JA, Reyna J, Bringas P, Thewissen JG, et al. Morphoregulation of teeth: modulating the number, size, shape and differentiation by tuning Bmp activity. Evol Dev 3 (2684). 2005;7(5):440-57.
28. Tapaltsyan V, Charles C, Hu J, Mindell D, Ahituv N, Wilson GM, et al. Identification of novel Fgf enhancers and their role in dental evolution. Evol Dev 3 (2684). 2016;18(1):31-40.
29. Thesleff I, Mikkola M. The role of growth factors in tooth development. Int Rev Cytol. 2002;217:93-135.
30. Tucker A, Sharpe P. The cutting-edge of mammalian development; how the embryo makes teeth. Nat Rev Genet 1 (39794). 2004;5(7):499-508.
31. Hu X, Lin C, Shen B, Ruan N, Guan Z, Chen Y, et al. Conserved odontogenic potential in embryonic dental tissues. J Dent Res 2 (4144). 2014;93(5):490-5.
32. Wang B, Li L, Du S, Liu C, Lin X, Chen Y, et al. Induction of human keratinocytes into enamel-secreting ameloblasts. Dev Biol. 2010;344(2):795-9.
33. Hu X, Lee JW, Zheng X, Zhang J, Lin X, Song Y, et al. Efficient induction of functional ameloblasts from human keratinocyte stem cells. Stem Cell Res Ther (4634). 2018;9(1):126.
34. Hu X, Zhang S, Chen G, Lin C, Huang Z, Chen Y, et al. Expression of SHH signaling molecules in the developing human primary dentition. Bmc Dev Biol 3 (2752). 2013;13:11.
35. Li CY, Prochazka J, Goodwin AF, Klein OD. Fibroblast growth factor signaling in mammalian tooth development. Odontology 4 (1354). 2014;102(1):1-13.
36. Cam Y, Neumann MR, Oliver L, Raulais D, Janet T, Ruch JV. Immunolocalization of acidic and basic fibroblast growth factors during mouse odontogenesis. Int J Dev Biol 3 (2567). 1992;36(3):381-9.
37. Huang F, Hu X, Fang C, Liu H, Lin C, Zhang Y, et al. Expression profile of critical genes involved in FGF signaling pathway in the developing human primary dentition. Histochem Cell Biol 3 (2927). 2015;144(5):457-69.
38. Kettunen P, Thesleff I. Expression and function of FGFs-4, -8, and -9 suggest functional redundancy and repetitive use as epithelial signals during tooth morphogenesis. Dev Dyn. 1998;211(3):256-68.
39. Baldin V, Lukas J, Marcote MJ, Pagano M, Draetta G. Cyclin D1 is a nuclear protein required for cell cycle progression in G1. Genes Dev. 1993;7(5):812-21.
40. Gartel AL, Radhakrishnan SK. Lost in transcription: p21 repression, mechanisms, and

consequences. Cancer Res 1 (9284). 2005;65(10):3980-5.
41. Cai J, Cho SW, Kim JY, Lee MJ, Cha YG, Jung HS. Patterning the size and number of tooth and its cusps. Dev Biol 3 (3637). 2007;304(2):499-507.
42. Jiang TX, Jung HS, Widelitz RB, Chuong CM. Self-organization of periodic patterns by dissociated feather mesenchymal cells and the regulation of size, number and spacing of primordia. Development 2 (6273). 1999;126(22):4997-5009.
43. Brewer JR, Mazot P, Soriano P. Genetic insights into the mechanisms of Fgf signaling. Genes Dev. 2016;30(7):751-71.
44. Lan Y, Jia S, Jiang R. Molecular patterning of the mammalian dentition. Semin Cell Dev Biol 2 (5971). 2014;25-26:61-70.
45. Abzhanov A, Tzahor E, Lassar AB, Tabin CJ. Dissimilar regulation of cell differentiation in mesencephalic (cranial) and sacral (trunk) neural crest cells in vitro. Development 2 (6273). 2003;130(19):4567-79.
46. Kratochwil K, Galceran J, Tontsch S, Roth W, Grosschedl R. FGF4, a direct target of LEF1 and Wnt signaling, can rescue the arrest of tooth organogenesis in Lef1(-/-) mice. Genes Dev. 2002;16(24):3173-85.
47. Kurosaka H, Islam MN, Kuremoto K, Hayano S, Nakamura M, Kawanabe N, et al. Core binding factor beta functions in the maintenance of stem cells and orchestrates continuous proliferation and differentiation in mouse incisors. Stem Cells 1 (7133). 2011;29(11):1792-803.
48. Jernvall J, Kettunen P, Karavanova I, Martin LB, Thesleff I. Evidence for the role of the enamel knot as a control center in mammalian tooth cusp formation: non-dividing cells express growth stimulating Fgf-4 gene. Int J Dev Biol 3 (2567). 1994;38(3):463-9.
49. Irazoqui AP, Boland RL, Buitrago CG. Actions of 1,25(OH)2-vitamin D3 on the cellular cycle depend on VDR and p38 MAPK in skeletal muscle cells. J Mol Endocrinol 2 (3621). 2014;53(3):331-43.
50. Vandomme J, Touil Y, Ostyn P, Olejnik C, Flamenco P, El Machhour R, et al. Insulin-like growth factor 1 receptor and p38 mitogen-activated protein kinase signals inversely regulate signal transducer and activator of transcription 3 activity to control human dental pulp stem cell quiescence, propagation, and differentiation. Stem Cells Dev 2 (4202). 2014;23(8):839-51.
51. Stockl S, Bauer RJ, Bosserhoff AK, Gottl C, Grifka J, Grassel S. Sox9 modulates cell survival and adipogenic differentiation of multipotent adult rat mesenchymal stem cells. J Cell Sci 2 (5325). 2013;126(Pt 13):2890-902.
52. Castellano E, Downward J. RAS Interaction with PI3K: More Than Just Another Effector Pathway. Genes Cancer. 2011;2(3):261-74.
53. Sun C, Zhao J, Jin Y, Hou C, Zong W, Lu T, et al. PTEN regulation of the proliferation and differentiation of auditory progenitors through the PTEN/PI3K/Akt-signaling pathway in mice. Neuroreport 4 (1644). 2014;25(3):177-83.
54. Xue XJ, Yuan XB. Nestin is essential for mitogen-stimulated proliferation of neural progenitor cells. Mol Cell Neurosci 2 (3734). 2010;45(1):26-36.
55. Michailovici I, Harrington HA, Azogui HH, Yahalom-Ronen Y, Plotnikov A, Ching S, et al. Nuclear to cytoplasmic shuttling of ERK promotes differentiation of muscle stem/progenitor cells. Development 2 (6273). 2014;141(13):2611-20.
56. Elledge SJ. Cell cycle checkpoints: preventing an identity crisis. Science 1 (31477). 1996;274(5293):1664-72.

57. Chambard JC, Lefloch R, Pouyssegur J, Lenormand P. ERK implication in cell cycle regulation. Biochim Biophys Acta. 2007;1773(8):1299-310.
58. Lin C, Yin Y, Bell SM, Veith GM, Chen H, Huh SH, et al. Delineating a conserved genetic cassette promoting outgrowth of body appendages. Plos Genet (8167). 2013;9(1):e1003231.
59. Zhang Y, Wang S, Song Y, Han J, Chai Y, Chen Y. Timing of odontogenic neural crest cell migration and tooth-forming capability in mice. Dev Dyn. 2003;226(4):713-8.
60. Song Y, Zhang Z, Yu X, Yan M, Zhang X, Gu S, et al. Application of lentivirus-mediated RNAi in studying gene function in mammalian tooth development. Dev Dyn. 2006;235(5):1334-44.
61. Hu X, Xu S, Lin C, Zhang L, Chen Y, Zhang Y. Precise chronology of differentiation of developing human primary dentition. Histochem Cell Biol 3 (2927). 2014;141(2):221-7.
62. St Amand TR, Zhang Y, Semina EV, Zhao X, Hu Y, Nguyen L, et al. Antagonistic signals between BMP4 and FGF8 define the expression of Pitx1 and Pitx2 in mouse tooth-forming anlage. Dev Biol 3 (3637). 2000;217(2):323-32.
63. Dong X, Shen B, Ruan N, Guan Z, Zhang Y, Chen Y, et al. Expression patterns of genes critical for BMP signaling pathway in developing human primary tooth germs. Histochem Cell Biol 3 (2927). 2014;142(6):657-65.
64. Xiong W, He F, Morikawa Y, Yu X, Zhang Z, Lan Y, et al. Hand2 is required in the epithelium for palatogenesis in mice. Dev Biol 3 (3637). 2009;330(1):131-41.
65. Yang G, Yuan G, Ye W, Cho KW, Chen Y. An atypical canonical bone morphogenetic protein (BMP) signaling pathway regulates Msh homeobox 1 (Msx1) expression during odontogenesis. J Biol Chem 2 (46). 2014;289(45):31492-502.